Effect of Zonal Flows on the Free Oscillations of a Barotropic Atmosphere

AKIRA KASAHARA

National Center for Atmospheric Research,[1] Boulder, CO 80307

(Manuscript received 27 September 1979, in final form 2 January 1980)

ABSTRACT

Solutions of the linearized global shallow-water equations (Laplace tidal equations) including the effect of a mean zonal flow are obtained by the Galerkin-transform method. Free oscillations of the first kind (gravity-inertia modes) are little affected by the zonal flow. Solutions of the second kind (rotational modes of the Rossby-Haurwitz type) are significantly affected by a zonal flow different from solid rotation. Only a few lowest rotational modes, whose angular phase velocities are less than the minimum velocity in the zonal flow, appear as discrete. The remaining angular phase velocities fall into a continuous spectrum which covers the interval between the minimum and maximum zonal velocities. An approximate, but accurate, frequency formula is obtained for the discrete modes of free oscillations under the effect of a mean zonal flow.

The frequencies and latitudinal structures of a few lowest rotational modes under the effect of a mean zonal flow are examined in detail and compared to observational evidence of westward propagating wavenumber 1 long-period oscillations in the atmosphere. The 5-day wavenumber 1 oscillation (the lowest symmetric rotational mode $l_R = 1$) is found insensitive to the presence of zonal flows. Other discrete modes are relatively sensitive to and their periods increased by the zonal flow effect. In particular, the period of the second symmetric rotational mode $l_R = 3$ (zonal wavenumber 1) increases to about 16–19 days in favor of the observations summarized by Madden (1978).

1. Introduction

In recent years, there have been many observational studies of traveling planetary waves in the atmosphere at long periods in excess of a few days. The largest scale in the longitudinal direction is referred to as zonal wavenumber 1. Despite differences in their data records and analysis techniques, many investigators found certain common characteristics of wavenumber 1 disturbances. The most well-known type propagates westward with periods of about 5 days in the troposphere (Deland, 1964; Eliasen and Machenhauer, 1965, 1969; Madden and Julian, 1972; Misra, 1975; Madden and Stokes, 1975) and in the stratosphere (Madden, 1975).[2] Another regular transient wavenumber 1 disturbance propagates westward with periods of 16–20 days in the troposphere (Eliasen and Machenhauer, 1965, 1969; Arai, 1970) and in the stratosphere (Hirota, 1975; Madden, 1975).

Eliasen and Machenhauer (1965) and Deland (1965) attempted to interpret these regular transient wavenumber 1 disturbances as westward propagating Rossby-Haurwitz waves based on the nondivergent vorticity equation over a sphere. They found discrepancies in the periods of oscillations, i.e., 3 and 10 days as the Haurwitz (1940) formula predicted versus near 5 and 18 days as they observed.

Dikiy and Golitsyn (1968) sought a possible cause of the above discrepancies in the effect of divergence in planetary-scale motions. They calculated the eigenfrequencies of the Laplace tidal equations with the equivalent height of 10 km and suggested that such discrepancies may be explained by taking into account the divergence effect and a correction due to the presence of background zonal flow. Eliasen and Machenhauer (1969) performed a similar study and arrived at essentially the same conclusion.

Madden (1978) presented further evidence for westward propagating wavenumber 1 disturbances with periods up to three weeks. Through the examination of the vertical and meridional distributions of the wave amplitudes, Madden concluded

[1] The National Center for Atmospheric Research is sponsored by the National Science Foundation.

[2] As discussed by Wallace and Chang (1969), this type of disturbance is different from that of westward propagating waves in the tropical lower stratosphere with 4–5 day periods and 10 000 km horizontal wavelengths as studied by Yanai and Maruyama (1966). The latter type of wave is antisymmetric with respect to the equator and is identified as the mixed Rossby-gravity wave in the terminology of Matsuno (1966). Wallace and Kousky (1968) reported on another type of wave disturbance with periods of about 15 days and wavelengths > 20 000 km. This type of wave is referred to as the atmospheric Kelvin wave (Holton and Lindzen, 1968). The transient waves with periods of 16–20 days discussed in this paper are not of the Kelvin type.

0022-4928/80/050917-13$07.25

that the westward propagating transient waves having periods of 5 days and near 16 days[3] are free oscillations of the external type with the equivalent height of 10 km in Laplace tidal equations.

Linearized equations governing oscillations of a stratified atmosphere at rest over a sphere can be separated into a horizontal structure and vertical structure equation. Free solutions of this system are referred to as the normal modes having discrete eigenfrequencies and the associated eigenfunctions. As Taylor (1936) showed, the horizontal structure of normal modes are the free solutions of linearized shallow-water equations, often referred to as Laplace's tidal equations with the separation constant h_e, called the equivalent height, being interpreted as a uniform depth of the homogeneous fluid.

The value of the equivalent height h_e is determined as an eigenvalue of the vertical structure equation satisfying the boundary conditions that vertical velocity vanish at the earth's surface and that kinetic energy at the top be finite. For a realistic temperature distribution of the atmosphere, it was found that the equivalent height h_e of $\sim$10 km is the only discrete eigenvalue (Butler and Small, 1963; Dikiy, 1965; Lindzen and Blake, 1972).[4]

Once the value of the equivalent height h_e is obtained, the horizontal structure of oscillations is determined as a free solution of Laplace's tidal equations which are linearized shallow-water equations over a sphere with reference to a resting basic state. In the case of zonal wavenumber $s \geq 1$, two different wave motions with distinct frequencies exist—eastward and westward propagating gravity-inertia waves, called first kind and westward propagating rotational waves of the Rossby-Haurwitz type, called second kind (Margules, 1893; Hough, 1898). Various aspects of the eigensolutions of Laplace's tidal equations are discussed in Dikiy (1965), Flattery (1967), Longuet-Higgins (1968) and Kasahara (1976).

As mentioned earlier, Madden (1978) hypothesized that the observed westward propagating planetary waves with periods up to three weeks are free oscillations of the external mode with the equivalent height of 10 km. Madden's theoretical considerations are based on the normal mode solutions of Laplace's tidal equations with reference to the basic state at rest. The period and the horizontal structure of the 5-day wave (wavenumber 1) agree well with those of the lowest symmetric mode ($l_R = 1$) of the second kind (Rossby-Haurwitz type). In a period range of one to three weeks, Madden found that the horizontal structure of 16-day wave agrees with that of the second lowest symmetric mode ($l_R = 3$), but the period expected from the normal mode solutions is 12.3 days in disagreement with 16 days as observed.

This discrepancy in periods between observed 16 days and "predicted" 12.3 days may be due to neglect of the background zonal flow. The agreement, on the other hand, in the 5-day wave periods may be due to the insensitivity of this particular mode of oscillations to the background zonal flow as suggested by Geisler and Dickinson (1976).

The purpose of this work is to investigate the normal modes of linearized shallow-water equations over a sphere by taking into account a climatological zonal flow and to determine the sensitivity of realistic zonal wind profiles on the period and the horizontal structure of free oscillations in the barotropic atmosphere. The approach is similar to Dikiy and Katayev (1971) who solved a linearized nondivergent vorticity equation over a sphere by taking into account the effect of zonal flows. A reference directly relevant to the present study is Dickinson and Williamson (1972) who calculated the normal modes of linearized shallow-water equations over a sphere including the effect of zonal flow by the use of the finite difference method. The present method of solution is spectral and an eigenvalue problem is formulated with application of the Galerkin-transform method.

In Section 2 we present the linearized shallow-water equations over a sphere with reference to a steady zonal flow as the basic state. Sections 3 and 4 provide a discussion of the method of solution in terms of the Galerkin-transform approach. A similar approach is used by Boyd (1978) to investigate the effects of latitudinal shear on equatorial waves. In Section 5 the results of calculations in terms of the frequencies and horizontal structures of the normal modes with emphasis on the effects of background zonal flow is described. Section 6 presents an approximate analytical expression for the frequency of discrete oscillations with zonal flow effects while both the discrete and continuous frequency spectra of rotational modes are discussed in Section 7. The frequency spectrum is discrete in the case of no mean zonal flow. The continuous spectrum of Rossby-Haurwitz type motions occurs in the presence of a background zonal flow. Conclusions are presented in Section 8.

2. Basic equations

The shallow-water equations over a sphere are expressed by

$$\frac{du}{dt} - \left(f + \frac{u}{a}\tan\phi\right)v + \frac{g}{a\cos\phi}\frac{\partial h}{\partial \lambda} = 0, \quad (2.1)$$

[3] The period of this oscillation varies in the range of 10–20 days as recognized by Madden (1978). We will, however, refer this mode to the 16-day wave according to the convention of Madden (1978).

[4] If a rigid top is placed at a finite altitude as an upper boundary, there are an infinite number of h_e as internal modes in addition to the external mode (Lindzen *et al.*, 1968). These internal modes constitute a continuous spectrum of h_e.

$$\frac{dv}{dt} + \left(f + \frac{u}{a}\tan\phi\right)u + \frac{g}{a}\frac{\partial h}{\partial \phi} = 0, \quad (2.2)$$

$$\frac{dh}{dt} + \frac{h}{a\cos\phi}\left[\frac{\partial u}{\partial \lambda} + \frac{\partial}{\partial \phi}(v\cos\phi)\right] = 0, \quad (2.3)$$

with

$$\frac{d}{dt} = \frac{\partial}{\partial t} + \frac{u}{a\cos\phi}\frac{\partial}{\partial \lambda} + \frac{v}{a}\frac{\partial}{\partial \phi},$$

where λ denotes longitude, ϕ latitude, t time, a represents a mean radius of the earth (constant), $f = 2\Omega\sin\phi$, where Ω is the earth's angular velocity of rotation (constant), g the acceleration of gravity (constant), u and v the eastward and northward components of horizontal velocity, and h the height of the free surface.

We assume that the motion can be represented by the sum of a steady flow and small-amplitude perturbations superimposed on the steady flow that depends on latitude only and are indicated by an overbar. Thus,

$$\left.\begin{aligned} u &= \bar{u}(\phi) + u'(\lambda,\phi,t), \\ v &= v'(\lambda,\phi,t), \\ h &= \bar{h}(\phi) + h'(\lambda,\phi,t), \end{aligned}\right\} \quad (2.4)$$

where a prime denotes a perturbation quantity.

We introduce the dimensionless variables

$$\left.\begin{aligned} \tilde{u} &= u'/(gh_e)^{1/2}, \quad \tilde{v} = v'/(gh_e)^{1/2} \\ \tilde{h} &= h'/h_e, \quad \tilde{t} = 2\Omega t \end{aligned}\right\} \quad (2.5)$$

and dimensionless parameters

$$\left.\begin{aligned} \tilde{\omega}(\phi) &= \bar{u}(\phi)/(2a\Omega\cos\phi) \\ \bar{H}(\phi) &= \bar{h}(\phi)/h_e \\ \gamma &= (gh_e)^{1/2}/(2a\Omega) \end{aligned}\right\}, \quad (2.6)$$

where h_e is a constant and is considered as the equivalent height mentioned in Introduction.

We further assume that the perturbation variables are expressed by

$$\begin{pmatrix} \tilde{u} \\ \tilde{v} \\ \tilde{h} \end{pmatrix} = \begin{pmatrix} \hat{u}(\phi) \\ \hat{v}(\phi) \\ \hat{h}(\phi) \end{pmatrix} \exp[i(s\lambda - \sigma\tilde{t})], \quad (2.7)$$

where s denotes the zonal wavenumber and σ is the dimensionless frequency scaled by 2Ω.

Substituting (2.4)–(2.7) into (2.1)–(2.3) and retaining only the first-order perturbation quantities, the linearized equations are written in the form

$$(\mathbf{A} - i\sigma\mathbf{I})\mathbf{W} + i\mathbf{B}\mathbf{W} = 0, \quad (2.8)$$

where $\mathbf{I}$ is the identity matrix,

$$\mathbf{W} = \begin{pmatrix} \hat{u} \\ \hat{v} \\ \hat{h} \end{pmatrix}, \quad (2.9)$$

$$\mathbf{A} = \begin{bmatrix} 0 & -\sin\phi & \dfrac{is\gamma}{\cos\phi} \\ \sin\phi & 0 & \gamma\dfrac{d}{d\phi} \\ \dfrac{is\gamma}{\cos\phi} & \dfrac{\gamma}{\cos\phi}\dfrac{d}{d\phi}[(\ )\cos\phi] & 0 \end{bmatrix}, \quad (2.10)$$

$$\mathbf{B} = \begin{bmatrix} \tilde{\omega}s & i\left(2\tilde{\omega}\sin\phi - \cos\phi\dfrac{d\tilde{\omega}}{d\phi}\right) & 0 \\ -i2\tilde{\omega}\sin\phi & \tilde{\omega}s & 0 \\ \dfrac{s\gamma(\bar{H}-1)}{\cos\phi} & -i\gamma\left\{\dfrac{d\bar{H}}{d\phi} + \dfrac{(\bar{H}-1)}{\cos\phi}\dfrac{d}{d\phi}[(\ )\cos\phi]\right\} & \tilde{\omega}s \end{bmatrix}. \quad (2.11)$$

If $\tilde{\omega}$ vanishes, so does **B**. In this case (2.8) reduces to the well-known Laplace's tidal equations without tide generating forces.

3. Solution of the linearized shallow-water equations

We employ the Galerkin approximation to solve Eq. (2.8). As the basis functions to represent the solution of (2.8), we adopt the solutions W_0 satisfying

$$(\mathbf{A} - i\sigma_0\mathbf{I})\mathbf{W}_0 = 0. \quad (3.1)$$

This is the well-known system of Laplace's tidal equations and its solutions have been discussed, for example, by Longuet-Higgins (1968). Using the notation of Kasahara (1976), the solutions of (3.1)

are given by

$$\mathbf{W}_0 = \Theta_r^s(\phi) = \begin{pmatrix} U_r^s(\phi) \\ -iV_r^s(\phi) \\ Z_r^s(\phi) \end{pmatrix}, \tag{3.2}$$

where s is the zonal wavenumber and r denotes the meridional index. We call $\Theta_r^s(\phi)$ the Hough vector functions after Hough (1898) who obtained the solutions of (3.1) by the spherical harmonic expansion. In (3.1), σ_0 is the associated frequency satisfying

$$\mathbf{A}\Theta_r^s = i(\sigma_r^s)_0\Theta_r^s. \tag{3.3}$$

In other words, $(\sigma_r^s)_0$ is an eigenvalue of Laplace tidal matrix $\mathbf{A}$ and Θ_r^s is the associated eigenvector. Both quantities are functions of wavenumber s and meridional index r.

In the case of $s \geq 1$, two different kinds of motions with distinct frequencies exist—eastward and westward propagating gravity-inertia waves (first kind) and westward propagating rotational waves of the Rossby-Haurwitz type (second kind). In the case of $s = 0$, the frequencies of gravity-inertia motions (first kind) appear as pairs of positive and negative values of the same magnitudes, and the frequencies of rotational motions (second kind) are all zero (Longuet-Higgins, 1968). We can construct solutions $\Theta_r^s(\phi)$ satisfying (3.1) and the orthogonality condition

$$\int_{-1}^{1} \Theta_r^s \cdot \Theta_{r'}^{s*} d\mu = \int_{-1}^{1} (U_r^s U_{r'}^s + V_r^s V_{r'}^s + Z_r^s Z_{r'}^s) d\mu = \delta_{rr'}, \tag{3.4}$$

where

$$\mu = \sin\phi, \tag{3.5}$$

the asterisk denotes the complex conjugate, and $\delta_{rr'} = 1$ if $r = r'$ and zero otherwise (Kasahara, 1978).

We now express the solution of (2.8) in terms of a series of Hough vector functions:

$$\mathbf{W}(\phi) = \sum_{r=1}^{\infty} C_r^s \Theta_r^s(\phi), \tag{3.6}$$

where C_r^s are the expansion coefficients.

Substituting (3.6) into (2.8) and using (3.3), we find

$$-i\sigma \sum_{r=1}^{\infty} C_r^s \Theta_r^s + \sum_{r=1}^{\infty} C_r^s i(\sigma_r^s)_0 \Theta_r^s + i\mathbf{B} \sum_{r=1}^{\infty} C_r^s \Theta_r^s = 0.$$

After application of inner product to the above equation by the complex conjugate of $\Theta_{r'}^s$, we integrate the resulting equation from the south to north poles with respect to μ ($\equiv \sin\phi$) and obtain

$$-\sigma \sum_{r=1}^{\infty} C_r^s \int_{-1}^{1} \Theta_r^s \cdot \Theta_{r'}^{s*} d\mu + \sum_{r=1}^{\infty} C_r^s (\sigma_r^s)_0 \int_{-1}^{1} \Theta_r^s \cdot \Theta_{r'}^{s*} d\mu + \int_{-1}^{1} (\mathbf{B} \sum_{r=1}^{\infty} C_r^s \Theta_r^s) \cdot \Theta_{r'}^{s*} d\mu = 0,$$

where the asterisk denotes the complex conjugate.

By the orthonomality condition (3.4), the above equation reduces to

$$[(\sigma_{r'}^s)_0 - \sigma] C_{r'}^s + \sum_{r=1}^{\infty} b_{r'r}^s C_r^s = 0, \qquad r' = 1, 2, \ldots, \tag{3.7}$$

where

$$b_{r'r}^s = \int_{-1}^{1} \mathbf{B}\Theta_r^s \cdot \Theta_{r'}^{s*} d\mu. \tag{3.8}$$

Since the series in (3.7) is infinite, we must truncate it to determine the expansion coefficients C_r^s. We define the vector

$$\mathbf{X} = (C_1^s, C_2^s, \ldots, C_R^s)^{\mathrm{T}}, \tag{3.9}$$

where R is a natural number, and the matrix

$$\mathbf{M} = \begin{bmatrix} [(\sigma_1^s)_0 + b_{11}^s] & b_{12}^s & \cdots & b_{1R}^s \\ b_{21}^s & [(\sigma_2^s)_0 + b_{22}^s] & \cdots & b_{2R}^s \\ b_{31}^s & b_{32}^s & \cdots & b_{3R}^s \\ \vdots & \vdots & & \vdots \\ b_{R1}^s & b_{R2}^s & \cdots & [(\sigma_R^s)_0 + b_{RR}^s] \end{bmatrix}. \tag{3.10}$$

We can write (3.7) as a standard eigenvalue-eigenfunction problem

$$(\mathbf{M} - \sigma\mathbf{I})\mathbf{X} = 0, \tag{3.11}$$

where σ is given as an eigenvalue of $\mathbf{M}$ and $\mathbf{X}$ as the associated eigenvector.

Next, we calculate the elements of **M**. With the aid of (2.11) and (3.2), we obtain

$$\mathbf{B}\Theta_r^s = \begin{pmatrix} \bar{\omega}sU_r^s + \left(2\bar{\omega}\sin\phi - \cos\phi\dfrac{d\bar{\omega}}{d\phi}\right)V_r^s \\ -i(2\bar{\omega}\sin\phi)U_r^s - i\bar{\omega}sV_r^s \\ \dfrac{s\gamma(\bar{H}-1)}{\cos\phi}U_r^s - \gamma\left[\dfrac{d\bar{H}}{d\phi}V_r^s + \dfrac{(\bar{H}-1)}{\cos\phi}\dfrac{d}{d\phi}(V_r^s\cos\phi)\right] + \bar{\omega}sZ_r^s \end{pmatrix}.$$

Then, the integral $b^s_{r',r}$ of (3.8) can be expressed as

$$b^s_{r',r} = \int_{-1}^{1}\left\{\bar{\omega}s(U_r^sU_{r'}^s + V_r^sV_{r'}^s + Z_r^sZ_{r'}^s) + 2\bar{\omega}\sin\phi(V_r^sU_{r'}^s + U_r^sV_{r'}^s) - \cos\phi\frac{d\bar{\omega}}{d\phi}V_r^sU_{r'}^s - \gamma\frac{d\bar{H}}{d\phi}V_r^sZ_{r'}^s + \frac{(\bar{H}-1)\gamma}{\cos\phi}\left[sU_r^s - \frac{d}{d\phi}(V_r^s\cos\phi)\right]Z_{r'}^s\right\}d\mu. \quad (3.12)$$

Once the elements C_r^s of eigenvector **X** of (3.11) are determined, the solution of (2.8) is obtained from the series (3.6) truncated at $r = R$. The accuracy of the solution will depend on the number R of truncation.

To calculate the elements $b^s_{r',r}$ of (3.12) in (3.10), we specify the form of $\bar{\omega}(\phi)$ and $\bar{H}(\phi)$ corresponding to the basic zonal flow which will be discussed in the next section.

4. Basic-state zonal flow

From (2.2) the relationship between the basic zonal flow $\bar{u}(\phi)$ and the corresponding height profile $\bar{h}(\phi)$, as given in (2.4), is expressed by

$$-\left(2\Omega\sin\phi + \frac{\bar{u}\sin\phi}{a\cos\phi}\right)\bar{u} = \frac{g}{a}\frac{d\bar{h}}{d\phi}. \quad (4.1)$$

In terms of dimensionless variables $\bar{\omega}(\phi)$ and $\bar{H}(\phi)$, defined in (2.6), Eq. (4.1) becomes

$$(1+\bar{\omega})\bar{\omega}\sin\phi\cos\phi = -\gamma^2\frac{d\bar{H}}{d\phi}. \quad (4.2)$$

By integrating (4.2) with respect to ϕ and taking into account the boundary condition that $\bar{H}(0) = 1$ at the equator, we find that

$$\bar{H}(\phi) = 1 - (2\gamma^2)^{-1}\int_0^{\phi}(1+\bar{\omega})\bar{\omega}\sin(2\phi)d\phi. \quad (4.3)$$

We express a given zonal wind profile $\bar{u}(\phi)$ as a function of latitude ϕ as

$$\bar{u}(\phi) = \sum_k r_k\cos(k\phi) + \sum_m r_m\sin(m\phi) \quad (4.4)$$

for $k = 1, 3, 5, \ldots, 17$ and $m = 2, 4, 6, \ldots, 18$, where

$$r_k = \frac{2}{\pi}\int_{-\pi/2}^{\pi/2}\bar{u}\cos(k\phi)d\phi$$

are the coefficients for the symmetric part of the series (4.4) and

$$r_m = \frac{2}{\pi}\int_{-\pi/2}^{\pi/2}\bar{u}\sin(m\phi)d\phi$$

are the coefficients for the antisymmetric part. Hence, $\bar{\omega}$, $d\bar{\omega}/d\phi$, $\bar{H}$ and $d\bar{H}/d\phi$ are calculated analytically.

To evaluate the matrix elements $b^s_{r',r}$, we need to construct the Hough vector functions U_l^s, V_l^s, Z_l^s and the derivative $d(V_l^s\cos\phi)/d\phi$ for given wavenumber s and meridional index l as functions of latitude. Since a general zonal flow $\bar{u}(\phi)$ is given from the south pole to the north pole, we must use both the symmetric and antisymmetric Hough vector functions to express solution $\mathbf{W}(\phi)$ of (3.6). The value of 10 km is chosen for the equivalent height h_e throughout the calculations.

From our experience of numerical integration of the global barotropic primitive equations with Hough harmonic expansions (Kasahara, 1977, 1978), it may be appropriate to use the total of 40 terms [the truncation $R = 40$ in (3.9)] including 20 symmetric modes ($l_{EG} = 0, 2, 4, 6; l_{WG} = 0, 2, 4, 6; l_R = 1, 3, 5, \ldots, 23$) and 20 antisymmetric modes ($l_{EG} = 1, 3, 5, 7; l_{WG} = 1, 3, 5; l_R = 0, 2, 4, \ldots, 24$) of Hough vector functions for zonal wavenumber $s \geq 1$. The accuracy of representing solutions by the series expansion will be judged by inspection of the spectral distribution of the expansion coefficients. Here, we use l_{EG}, l_{WG} and l_R to distinguish the meridional indices of eastward and westward propagating gravity modes from rotational modes. Frequency $(\sigma_l^s)_0$ is associated with each Hough vector function Θ_l^s.

To calculate the integral (3.12), we use the Gaussian quadrature formula which is exact for any polynomial of degree smaller than or equal to $2K - 1$, when we use the formula with K latitude points between the south pole to the north pole (e.g., Hildebrand, 1956). We found that it is sufficient to use $K = 64$.

Once the elements of the matrix **M** of (3.10) are

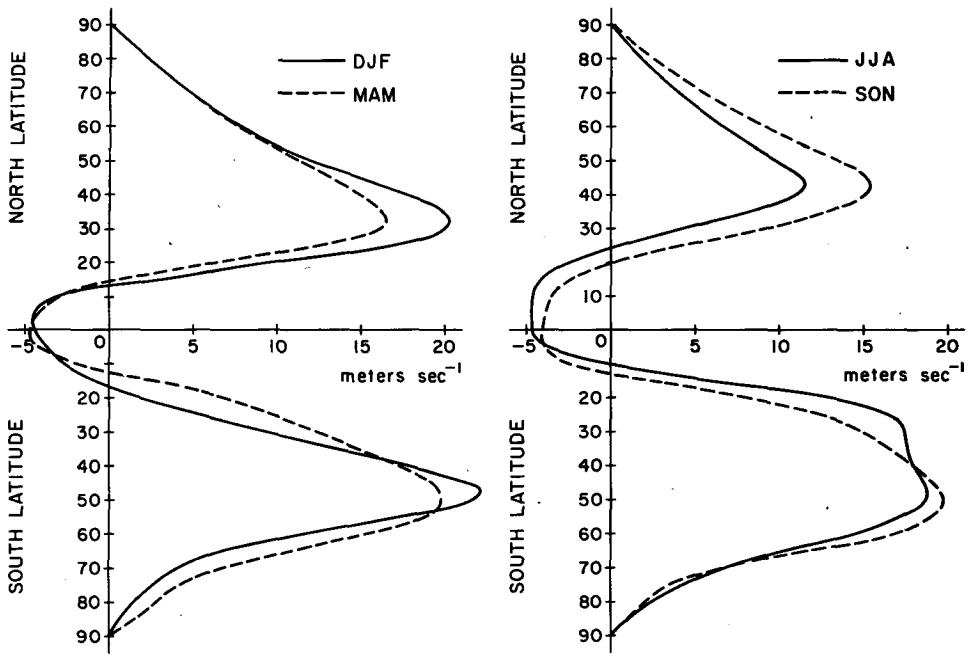

FIG. 1. Climatological zonal wind distributions at 500 mb after Crutcher (1961) and van Loon *et al.* (1971) for four seasons—December, January, February (DJF), March, April, May (MAM), June, July, August (JJA), and September, October, November (SON).

TABLE 1. Periods of oscillation in days of several lowest rotational modes.

l_R	No zonal flow	DJF	MAM	JJA	SON
		Zonal wavenumber s = 1			
0	1.19	1.20	1.20	1.20	1.20
1	5.02	4.85	4.87	4.85	4.85
2	8.30	9.91	9.99	9.49	9.52
3	12.32	18.39	17.22	16.68	17.40
4	17.29	28.08	26.50	24.78	27.09
		Zonal wavenumber s = 2			
0	1.62	1.71	1.71	1.69	1.70
1	3.74	3.84	3.84	3.79	3.84
2	5.93	7.27	7.55	6.93	7.07
3	8.51	14.23	13.54	12.71	13.22
4	11.54	21.47	20.60	18.39	20.03
		Zonal wavenumber s = 3			
0	2.08	2.30	2.29	2.25	2.26
1	3.72	4.28	4.22	4.10	4.22
2	5.52	7.40	7.60	6.73	7.06
3	7.59	13.65	13.89	11.78	12.76
		Zonal wavenumber s = 4			
0	2.56	2.90	2.90	2.79	2.82
1	3.99	5.21	5.03	4.80	4.97
2	5.59	8.20	8.22	7.18	7.69
3	7.40	13.55	13.84	11.18	12.44

calculated, the eigenvalues σ and the associated eigenvectors **X** are obtained from the square matrix **M** of order 40 using a standard eigenvalue-eigenfunction routine.

5. Frequency and latitudinal structure of normal modes with the zonal flow effect

As a representative mean zonal wind profile appropriate to the barotropic atmosphere, we choose the climatological zonal wind distributions at 500 mb after Crutcher (1961) and van Loon *et al.* (1971). The 500 mb level may be considered to be a good approximation to the equivalent barotropic level (Charney, 1949). Fig. 1 shows the four mean zonal wind distributions corresponding to four seasons—December, January, February (DJF), March, April, May (MAM), June, July, August (JJA), and September, October, November (SON).

Table 1 lists the period of oscillation in days of several lowest rotational modes (l_R = 0, 1, . . .) for the cases of no zonal flow and zonal flows for four seasons, DJF, MAM, JJA and SON corresponding to zonal wavenumbers 1–4. Since the basic zonal flow has a latitudinal shear, the frequency σ of oscillations will not necessarily be real. However, as we will discuss later, the frequencies of these lowest rotational modes are all real. Moreover, these are westward propagating modes and the frequencies are negative.

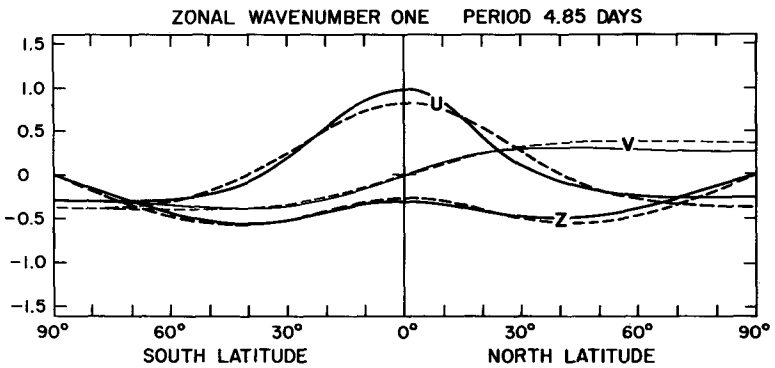

FIG. 2. Latitudinal structure of the normal mode of the rotational mode $l_R = 1$ and $s = 1$ with and without the zonal wind effect. Dashed lines represent the latitudinal structures of zonal wind component U_l^s, meridional wind component V_l^s, and free surface height Z_l^s in the case of no zonal flow. Solid lines show the latitudinal structures of the normal mode in the case of zonal wind profile of DJF.

For zonal wavenumber $s = 1$, the effect of zonal flow increases the periods of oscillations except for the $l_R = 1$ mode. The $l_R = 1$ mode has a period of 5.02 days without zonal flow, but it shortens slightly to 4.85–4.87 days with the zonal flow effect. For both the $l_R = 0$ and 1 modes, the periods of oscillations are insensitive to the variation of the zonal flow. The $l_R = 3$ mode has a period of 12.32 days without zonal flow, but it increases to 16–19 days due to the zonal flow effect.

Dickinson and Williamson (1972) calculated using a finite-difference method the frequencies of the rotational modes $l_R = 0$, 1, 2, 3 and 4 for $s = 1$ by assuming a symmetric zonal wind profile whose distribution is comparable to those used in the present calculations. They obtained the periods of 1.21, 5.05, 10.81, 17.61 and 32.18 days which are in agreement with those listed for $s = 1$ in the zonal flow cases. We will discuss in Section 6 why the period of $l_R = 1$ mode decreased in the present calculations while Dickinson and Williamson obtained a slight increase.

For the cases of zonal wavenumber $s \geq 2$ in Table 1, the zonal flow effect always increases the periods of oscillations with respect to the cases of no zonal flow.

Fig. 2 shows the latitudinal structure of the normal mode of $l_R = 1$ and $s = 1$ with and without the zonal flow. The abscissa denotes the latitude from the south pole to the north pole. Dashed lines represent the latitudinal structures of zonal wind component U_l^s, meridional wind component V_l^s, and free surface height Z_l^s in the case of no zonal flow. Solid lines show the latitudinal structures of the normal mode in the case of zonal wind profile of DJF. The differences in the latitudinal structures of the normal modes with and without the zonal flow effect are relatively small.

Fig. 3 shows the same as Fig. 2 except for the mode $l_R = 3$ and $s = 1$. As shown by the solid line for U, the zonal flow effect gives a substantial change in the zonal wind component U_l^s particularly in the tropics. Also, some differences exist in the structure of the normal mode in the Northern and Southern

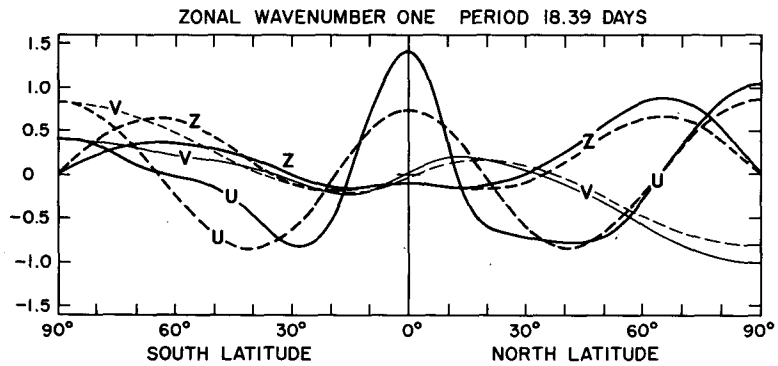

FIG. 3. As in Fig. 2 except for the rotational mode $l_R = 3$ and $s = 1$.

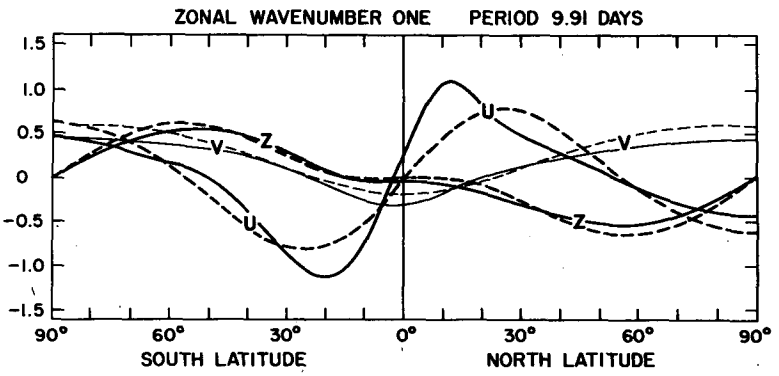

FIG. 4. As in Fig. 2 except for the rotational mode $l_R = 2$ and $s = 1$.

Hemispheres due to the differences in the zonal wind profiles in the two hemispheres.

Fig. 4 shows the same as Fig. 2 except for the mode $l_R = 2$ and $s = 1$ which is antisymmetric without the zonal flow effect. Again a noticeable change occurs in the latitudinal structure of zonal wind component U_l^s with the zonal flow effect.

TABLE 2. Comparison of the calculated frequency obtained from (3.11) with the approximate frequency given by formula (6.1).

	Frequency		$\Delta\sigma = \sigma - \sigma_0$	
	σ_0 No zonal flow	σ DJF	$\Delta\sigma$ DJF	Approximate $\Delta\sigma$ DJF
l_{EG}				
7	2.94579	2.91685	−0.02894	−0.02960
6	2.61513	2.59346	−0.02167	−0.02177
5	2.28566	2.27324	−0.01242	−0.01214
4	1.95697	1.95465	−0.00232	−0.00244
3	1.62663	1.63516	0.00853	0.00816
2	1.28440	1.29728	0.01288	0.01261
1	0.89361	0.89850	0.00489	0.00478
0	0.37056	0.37438	0.00382	0.00357
l_{WG}				
6	−2.63446	−2.58356	0.05090	0.05136
5	−2.31214	−2.26816	0.04398	0.04421
4	−1.99571	−1.95854	0.03717	0.03669
3	−1.68932	−1.66030	0.02902	0.02874
2	−1.40273	−1.38415	0.01858	0.01858
1	−1.15168	−1.14843	0.00325	0.00352
0	−0.90793	−0.90577	0.00216	0.00232
l_R				
0	−0.42147	−0.41609	0.00538	0.00515
1	−0.09959	−0.10305	−0.00346	−0.00330
2	−0.06024	−0.05046	0.00978	0.01167
3	−0.04060	−0.02719	0.01341	0.01506
4	−0.02892	−0.01781	0.01111	0.01456
5	−0.02149	−0.01035	0.01114	0.01447
6	−0.01653	−0.00702	0.00951	0.01252
7	−0.01308	−0.00498	0.00810	0.01344
8	−0.01059	−0.00338	0.00721	0.01362
.	.	.	.	.
.	.	.	.	.
.	.	.	.	.

6. Approximate frequency formula for free oscillations with zonal flow effect

Assuming the dominance of the diagonal elements of matrix (3.10), we derive the following frequency formula for free oscillations with the zonal flow effect:

$$\sigma_r^s \approx (\sigma_r^s)_0 + \Delta\sigma_A + \Delta\sigma_M + \Delta\sigma_H + \Delta\sigma_D, \quad (6.1)$$

where

$$\Delta\sigma_A = \int_{-1}^{1} \tilde{\omega} s[(U_r^s)^2 + (V_r^s)^2 + (Z_r^s)^2]d\mu, \quad (6.2)$$

$$\Delta\sigma_c = \int_{-1}^{1} \left(4\tilde{\omega}\sin\phi - \cos\phi \frac{d\tilde{\omega}}{d\phi}\right) V_r^s U_r^s d\mu, \quad (6.3)$$

$$\Delta\sigma_H = -\int_{-1}^{1} \gamma \frac{d\tilde{H}}{d\phi} V_r^s Z_r^s d\mu, \quad (6.4)$$

$$\Delta\sigma_D = \int_{-1}^{1} \frac{(\tilde{H} - 1)\gamma}{\cos\phi} \times \left[sU_r^s - \frac{d}{d\phi}(V_r^s \cos\phi)\right] Z_r^s d\mu. \quad (6.5)$$

Formula (6.1) consists of the frequency $(\sigma_r^s)_0$ without a zonal flow and the four correction terms (6.2)–(6.5). These correction terms due to the zonal flow effect may be referred to as, respectively, advective, Coriolis, free surface height slope and divergence effects.

To check the accuracy of formula (6.1), Table 2 compares the calculated frequency σ obtained from (3.11) with the approximate σ given by (6.1) for both the gravity-inertia and rotational modes. The first column indicates the meridional index of modes. The second column shows the corresponding frequency σ_0 without zonal flow effects. The third denotes the frequency σ calculated from (3.11) with

the zonal flow of DJF. The fourth and fifth columns, respectively, are the difference $\Delta\sigma$ as given by the third column minus the second column and the approximate $\Delta\sigma$ as given by the sum of (6.2)–(6.5). A comparison between the fourth and fifth columns show that the approximate formula (6.1) is accurate for the gravity-inertia modes and the lowest two rotational modes, but the accuracy of approximation deteriorates for higher rotational modes.

Table 3 shows the values of individual correction terms $\Delta\sigma_A$ through $\Delta\sigma_D$ for several lowest rotational modes for $s = 1$ with the DJF zonal flow. The first column denotes the meridional index l_R. The second column shows the sum of the four correction terms $\Delta\sigma_A$ through $\Delta\sigma_D$. The magnitude of $\Delta\sigma_D$ is generally small for the rotational modes, though this contribution is relatively large for the gravity-inertia modes. The height slope effect $\Delta\sigma_H$ is generally on the same order of magnitude of the Coriolis effect $\Delta\sigma_C$. The reason that the $l_R = 1$ mode has a negative value of $\Delta\sigma$ may be explained by the dominance of two negative terms $\Delta\sigma_C$ and $\Delta\sigma_H$ over the positive advective effect $\Delta\sigma_A$. In the calculation of Dickinson and Williamson (1972) for the same mode referred to in Section 5, both the height slope and divergence effects were not included. The insensitivity of the 5-day wave oscillations with respect to the background wind may be explained by the approximate cancellation of the advective effect by the Coriolis effect.

7. Discrete and continuous frequency spectra of the rotational modes

So far we have examined only a few of the lowest rotational modes. In this section, we will discuss all of the rotational modes obtained as the solutions of (3.11). Dikiy and Katayev (1971) investigated the solutions of the linear nondivergent vorticity equation over a sphere. If small perturbations are superimposed on a zonal flow different from a solid rotation, then of the infinite spectrum of Rossby-Haurwitz waves there remain only a finite number of discrete modes whose angular phase velocities are less than the minimum velocity of the zonal flow; the rest merge into a continuous spectrum that covers the interval between the minimum and maximum velocities of the zonal flow. A similar situation arises in the case of rotational modes of Laplace tidal equations when the effect of a zonal flow different from a solid rotation is considered. On the other hand, the gravity-inertia modes are little affected by the effect of zonal flow.

TABLE 3. Values of individual correction terms $\Delta\sigma_A$ through $\Delta\sigma_D$ for several lowest rotational modes for zonal wavenumber $s = 1$ with the DJF zonal flow.

l_R	$\Delta\sigma$	$\Delta\sigma_A$	$\Delta\sigma_C$	$\Delta\sigma_H$	$\Delta\sigma_D$
0	0.00515	0.01122	−0.00214	−0.00506	0.00113
1	−0.00330	0.01045	−0.00828	−0.00634	0.00088
2	0.01167	0.01642	0.00029	−0.00580	0.00075
3	0.01506	0.01583	0.00232	−0.00352	0.00043
4	0.01456	0.01506	0.00155	−0.00228	0.00023

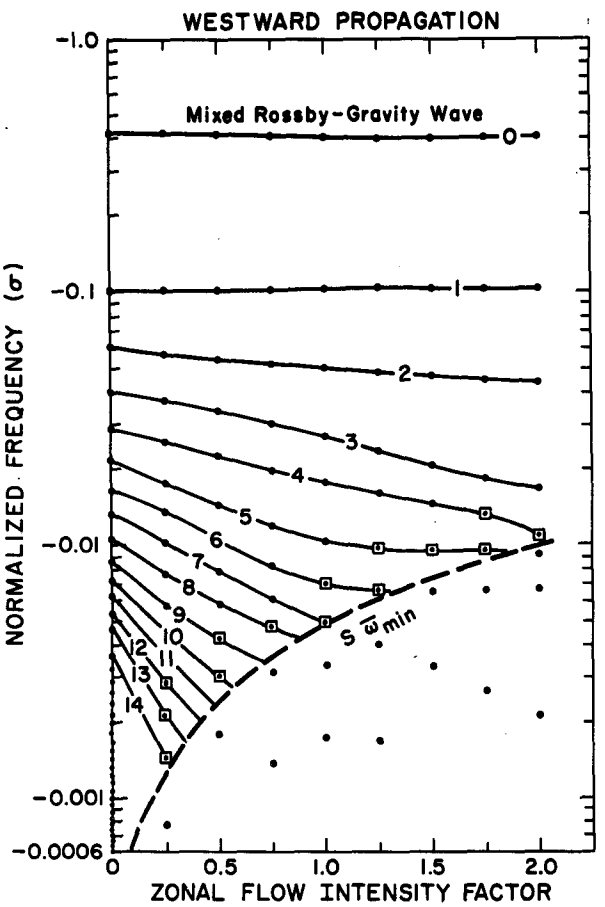

FIG. 5. Dimensionless frequency σ of the rotational modes for zonal wavenumber $s = 1$ obtained as the solutions of (3.11). The abscissa is the intensity factor α for the mean zonal flow $\bar{\omega}(\phi)$ based on the DJF profile. Solutions of (3.11) are obtained by assuming the mean zonal wind $\alpha\bar{\omega}(\phi)$. The real parts of frequencies σ of the rotational modes are plotted in 0.25 increments of α. Negative frequencies for westward propagation are plotted. The dots in the continuous spectrum have no physical significance, but they are plotted merely to show what Galerkin's method gives when one tries to represent singular, continuum modes in terms of a finite set of Hough vector functions.

On Figs. 5 and 6, we have plotted the real part of frequency σ of the rotational modes for zonal wavenumber $s = 1$ obtained as the solutions of (3.11) when the various intensities of the mean zonal flow are assumed. (As we explain later, the data points which are associated with complex eigenvalues are denoted by the circles in Fig. 6.) The abscissa is the intensity factor α for the mean zonal flow $\bar{\omega}(\phi)$ based on the DJF profile. The solutions of

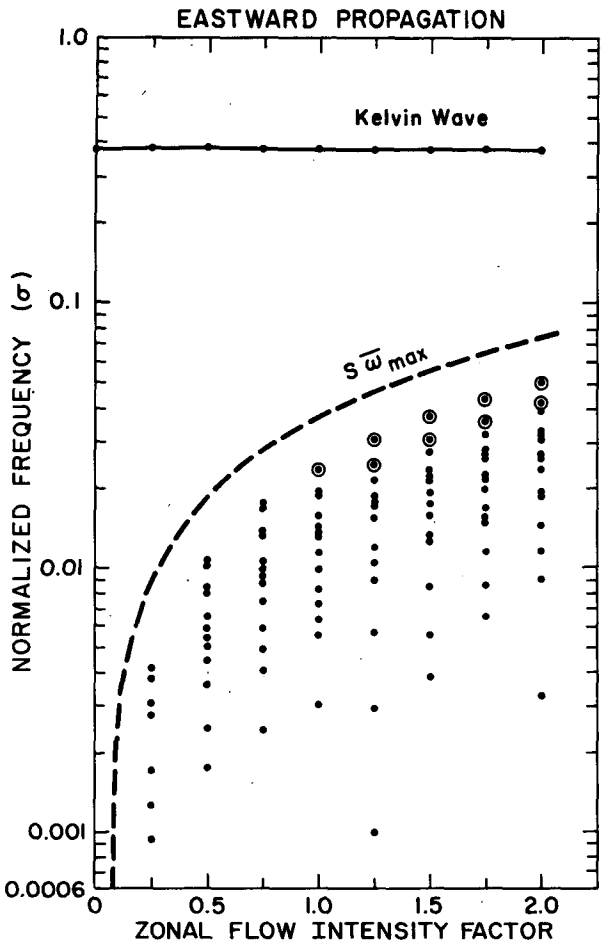

FIG. 6. As in Fig. 5 except for the positive frequencies for eastward propagation.

(3.11) were obtained by assuming the mean zonal flow given by $\alpha\bar{\omega}(\phi)$. Negative real frequencies for westward propagation are plotted on Fig. 5 and positive real frequencies for eastward propagation on Fig. 6. The number labeled on the solid lines in Fig. 5 denotes the meridional index l_R of rotational modes.

In the case of no zonal flow ($\alpha = 0$), all the rotational modes are discrete. When α increases, because of the zonal flow effect, the higher rotational modes whose frequencies are larger than $s\bar{\omega}_{min}$, where $\bar{\omega}_{min}$ is the minimum of $\bar{\omega}(\phi)$ and s is the zonal wavenumber ($s = 1$ in this case), are no longer discrete and fall in the continuous spectrum. The continuous spectrum covers the interval between $s\bar{\omega}_{min}$, shown by the dashed line in Fig. 5, and $s\bar{\omega}_{max}$ shown by the dashed line in Fig. 6, where $\bar{\omega}_{max}$ denotes the maximum of $\bar{\omega}(\phi)$. At some point in this interval, the real part of the phase velocity coincides with the zonal velocity and this point is referred to as a critical level. Because of the singularity, the normal mode solution shows a sharp variation through the critical level. It is difficult to represent the solutions in terms of discrete grid-functions or a finite series of functions unless a large number of resolutions are employed. The dots shown in the continuous spectrum have no physical significance, but they are plotted merely to show what the present calculation gives. For more information on different types of normal modes of parallel flow in inviscid stratified fluids, see, for example, Banks *et al.* (1976).

In Fig. 5, the solid lines are drawn by connecting the discrete spectrum points of the same meridional indices for various values of α. The frequency values of lower rotational modes, $l_R = 0, 1, 2, 3$, in particular, and higher rotational modes for small values of α are determined accurately as the magnitudes of the expansion coefficients C_r^s of (3.6) fall off rather sharply in those cases. On the other hand, the frequency values enclosed by the squares are not considered reliable because the magnitudes of the expansion coefficients do not fall rapidly so that there is some question concerning the sufficiency of a total of 40 terms of the expansion coefficients. Since our interest is in the lower rotational modes, the question on the accuracy of data points enclosed by the squares was not pursued further.

In the case of the nondivergent vorticity equation over a sphere, Dikiy and Katayev (1971) discuss the application of the Rayleigh-Kuo theorem (Kuo, 1949), i.e., there are no non-real frequencies until

$$1 - d^2[(1 - \mu^2)\bar{\omega}(\phi)]/d\mu^2$$

changes sign between the north and south poles. We calculated the above criterion for the zonal wind profiles used for the calculations referred to in Figs. 5 and 6. We found that the instability condition is satisfied for the wind profiles beyond $\alpha \geq 1.0$ in the search for conditions with an increment of $\alpha = 0.25$. The data points which are associated with complex eigenvalues are denoted by the circles in Fig. 6. The magnitudes of the imaginary part of frequency σ are generally very small. In terms of the exponential growth rate, the time required for the amplitude to grow by the factor of e is in the range 26–100 days.

8. Conclusions

Normal modes of the Laplace tidal equations including the effect of a mean zonal flow are obtained and the sensitivity of various zonal flow distributions on the period and the horizontal structure of free oscillations is examined. Solutions of the linearized global shallow-water equations with the effect of a mean zonal flow are expressed by a series of Hough vector functions of a given zonal wavenumber. Hough vector functions are the normal modes of Laplace tidal equations without the zonal

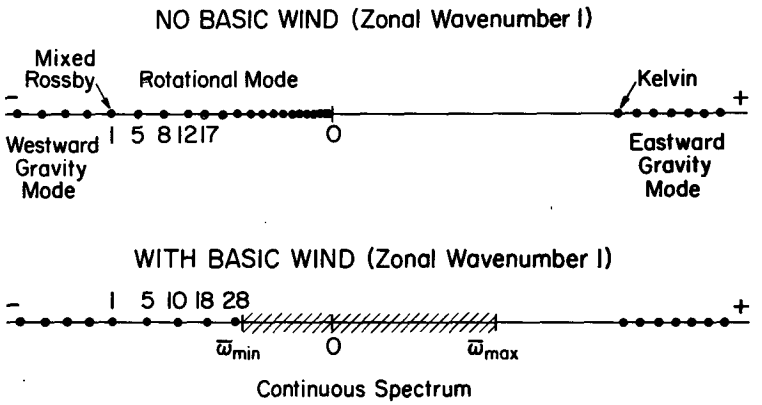

FIG. 7. The dots in the upper figure show the frequencies in the case of no background zonal flow. All the frequencies are discrete and are divided into the three species: westward gravity-inertia, eastward gravity-inertia and rotational. The numerals beside the dots in the rotational mode show approximate periods in days. The lower figure shows the modification of frequencies by the background flow. $\tilde{\omega}_{min}$ is the minimum of $\tilde{\omega}(\phi)$ and $\tilde{\omega}_{max}$ the maximum of $\tilde{\omega}(\phi)$, the angular velocity of the basic zonal flow.

flow effect. An eigenvalue problem is formulated by application of the Galerkin-transform method. As one advantage of the spectral method over the finite-difference method, we obtain an approximate, but accurate, analytical formula for the frequency of discrete modes of oscillations under the effect of a mean zonal flow. Such a formula will throw light on the nature of the zonal flow effect.

Fig. 7 illustrates schematically the modification of wave frequencies by the background zonal flow. The dots in the upper figure show the frequencies in the case of no background zonal flow. All the frequencies are discrete and are divided into the three species: westward gravity-inertia, eastward gravity-inertia and rotational. The numerals beside the dots in the rotational mode show approximate periods in days. Note a denumerable discrete spectrum of negative frequencies accumulating toward zero. The lower figure shows the modification of frequencies by the background flow.

Free oscillations of the first kind (gravity-inertia modes) are little affected by the presence of a mean zonal flow. Normal modes of the second kind (rotational mode) are significantly affected by a zonal flow with latitudinal shear. Only a few lowest rotational modes, whose angular phase velocities are less than the minimum velocity in the zonal flow, appear as discrete. The rest fall into a continuous spectrum which covers the interval between the minimum and maximum zonal velocities. The numerals beside the dots show the approximate frequencies in days modified under the DJF zonal wind profile.

The frequencies and latitudinal structures of a few lowest rotational modes are examined in view of observational evidences of westward propagating wavenumber 1 oscillations in the atmosphere summarized in Section 1. By recognizing the correspondence between the $l_R = 1$ mode with wavenumber $s = 1$ and the so-called 5-day wave, the present calculations seem to support the hypothesis by Geisler and Dickinson (1976) that the period and the latitudinal structure of this particular wave change very little by the present of zonal winds. On the other hand, the presence calculations show that the period of $l_R = 3$ mode with $s = 1$ increased from 12.3 days without a zonal flow to 16–19 days depending on the various profiles of the zonal flow. This result is favorable in explaining the discrepancy in periods between the observation and the "prediction" for this mode discussed in the Introduction.

The investigation on the free oscillations of the atmosphere under a realistic background zonal wind distribution requires solutions of a nonseparable three-dimensional atmospheric model. The present study is only the first step toward this goal which examines the effect of latitudinal shear of a mean zonal flow in a barotropic atmosphere. (An extension of the present approach to a multilayer baroclinic model is in progress.) Although the comparison between the present results and the observational evidences must be made with the model limitations in mind, the present results will be useful for providing a guidance to the analysis of atmospheric records. For example, while the existence of the two lowest symmetric rotational modes ($l_R = 1$ and 3) with wavenumber 1 is extensively investigated, the possibility of existence of the second antisymmetric mode ($l_R = 2$) with wavenumber 1 has not been questioned. The period of oscillation of the second antisymmetric mode

($l_R = 2$) with wavenumber 1 is expected to be about 10 days with the effect of mean zonal flows. Hirota (1976) detected clearly the presence of 10-day period westward propagating wavenumber 1 waves in the Nimbus 5 Selective Chopper Radiometer data in the stratosphere. A similar finding is reported by Rodgers (1976). However, it is not known whether those 10-day period waves observed by Hirota and Rodgers are of antisymmetric type or not. The identification of such a mode may require simultaneous data in the Northern and Southern Hemispheres. The normal mode structure shown in Fig. 4 will be useful to guide an analysis procedure. If the antisymmetric mode were found not to exist in the atmosphere, this would raise an interesting question as to the excitation mechanism of the two lowest symmetric rotational modes. It is beyond the scope of this present study to consider the mechanism of excitation of long-period free oscillations in the atmosphere.

Acknowledgments. The author thanks R. Daley, R. Dickinson, J. Gary, R. Madden, H. van Loon and D. Williamson for discussions and useful comments on this work. The manuscript was typed by Mary Niemczewski.

REFERENCES

Arai, Y., 1970: A statistical study of ultra-long waves. *J. Meteor. Soc. Japan*, **48**, 469–478.

Banks, W. H. H., P. G. Drazin and M. B. Zaturska, 1976: On the normal modes of parallel flow of inviscid stratified fluid. *J. Fluid Mech.*, **75**, 149–171.

Boyd, J. P., 1978: The effects of latitudinal shear on equatorial waves, Part I: Theory and methods. *J. Atmos. Sci.*, **35**, 2236–2258.

Butler, S. T., and K. A. Small, 1963: The excitation of atmospheric oscillations. *Proc. Roy. Soc. London*, **A274**, 91–121.

Charney, J. G., 1949: On a physical basis for numerical prediction of large-scale motions in the atmosphere. *J. Meteor.*, **6**, 371–385.

Crutcher, H. L., 1961: Meridional cross-sections of upper winds over the Northern Hemisphere. Tech. Pap. No. 41, U.S. Weather Bureau, Department of Commerce, Washington, D.C. 307 pp. [See *Meteorological Abstracts and Bibliography*, **13** (1962), 2135 pp. (13.8-41, 551.501.75: 551.557.2)].

Deland, R. J., 1964: Travelling planetary waves. *Tellus*, **16**, 271–273.

——, 1965: Some observations of the behavior of spherical harmonic waves. *Mon. Wea. Rev.*, **93**, 307–312.

Dickinson, R. E., and D. L. Williamson, 1972: Free oscillations of a discrete stratified fluid with application to numerical weather prediction. *J. Atmos. Sci.*, **29**, 623–640.

Dikiy, L. A., 1965: The terrestrial atmosphere as an oscillating system. *Izv. Atmos. Oceanic Phys.*, **1**, 275–286.

——, and G. S. Golitsyn, 1968: Calculation of the Rossby wave velocities in the earth's atmosphere. *Tellus*, **20**, 314–317.

——, and V. V. Katayev, 1971: Calculation of the planetary wave spectrum by the Galerkin method. *Izv. Atmos. Oceanic Phys.*, **7**, 1031–1038.

Eliasen, E., and B. Machenhauer, 1965: A study of the fluctuations of the atmospheric planetary flow patterns represented by spherical harmonics. *Tellus*, **17**, 220–238.

——, and ——, 1969: On the observed large-scale atmospheric wave motion. *Tellus*, **21**, 149–166.

Flattery, T. W., 1967: Hough functions. Tech. Rep. 21, Dept. Geophys. Sci., The University of Chicago, 175 pp.; also Ph.D. thesis, The University of Chicago.

Geisler, J. E., and R. E. Dickinson, 1976: The five-day wave on a sphere with realistic zonal winds. *J. Atmos. Sci.*, **33**, 632–641.

Haurwitz, B., 1940: The motion of atmospheric disturbances on the spherical earth. *J. Mar. Res.*, **3**, 254–267.

Hildebrand, F. B., 1956: *Introduction to Numerical Analysis*. McGraw-Hill, 511 pp.

Hirota, I., 1975: Spectral analysis of planetary waves in the summer stratosphere and mesosphere. *J. Meteor. Soc. Japan*, **53**, 33–44.

——, 1976: Seasonal variation of planetary waves in the stratosphere observed by the Nimbus 5 SCR. *Quart. J. Roy. Meteor. Soc.*, **102**, 757–770.

Holton, J. R., and R. S. Lindzen, 1968: A note on Kelvin waves in the atmosphere. *Mon. Wea. Rev.*, **96**, 385–386.

Hough, S. S., 1898: On the application of harmonic analysis to the dynamical theory of the tides, Part II: On the general integration of Laplace's dynamical equations. *Phil. Trans. Roy. Soc. London*, **A191**, 139–185.

Kasahara, A., 1976: Normal modes of ultralong waves in the atmosphere. *Mon. Wea. Rev.*, **104**, 669–690.

——, 1977: Numerical integration of the global barotropic primitive equations with Hough harmonic expansions. *J. Atmos. Sci.*, **34**, 687–701.

——, 1978: Further studies on a spectral model of the global barotropic primitive equations with Hough harmonic expansions. *J. Atmos. Sci.*, **35**, 2043–2051.

Kuo, H.-L., 1949: Dynamic instability of two-dimensional nondivergent flow in a barotropic atmosphere. *J. Meteor.*, **6**, 105–122.

Lindzen, R. S., and D. Blake, 1972: Lamb waves in the presence of realistic distributions of temperature and dissipation. *J. Geophys. Res.*, **77**, 2166–2176.

——, E. S. Batten, and J.-W. Kim, 1968: Oscillations in atmospheres with tops. *Mon. Wea. Rev.*, **96**, 133–140.

Longuet-Higgins, M. S., 1968: The eigenfunctions of Laplace's tidal equations over a sphere. *Phil. Trans. Roy. Soc. London*, **A262**, 511–607.

Madden, R., 1975: Oscillations in the winter stratosphere, Part 2: The role of horizontal eddy heat transport and the interaction of transient and stationary planetary waves. *Mon. Wea. Rev.*, **103**, 717–729.

——, 1978: Further evidence of traveling planetary waves. *J. Atmos. Sci.*, **35**, 1605–1618.

——, and P. R. Julian, 1972: Further evidence of global-scale 5-day pressure waves. *J. Atmos. Sci.*, **29**, 1464–1469.

——, and J. Stokes, 1975: Evidence of global-scale 5-day waves in a 73-year pressure record. *J. Atmos. Sci.*, **32**, 831–836.

Margules, M., 1893: Luftbewegungen in einer rotierenden Sphäroidschale. Teil. II. *S.-B. Akad. Wiss. Wien, Math.-Naturwiss I., Abt. IIa*, **102**, 11–56.

Matsuno, T., 1966: Quasi-geostrophic motions in the equatorial area. *J. Meteor. Soc. Japan*, **44**, 25–43.

Misra, B. M., 1975: Evidence of the 5-day period oscillations in the geopotential field. *Tellus*, **27**, 469–483.

Rodgers, C. D., 1976: Evidence for the five-day wave in the upper stratosphere. *J. Atmos. Sci.*, **33**, 710–711.

Taylor, G. I., 1936: The oscillations of the atmosphere. *Proc. Roy. Soc. London*, **A156**, 318–326.

van Loon, H., J. J. Taljaard, R. L. Jenne, and H. L. Crutcher, 1971: *Climate of the Upper Air: Southern Hemisphere*, Vol. II: *Zonal Geostrophic Winds*. NAVAIR 50-IC-56 [Na-

tional Climatic Center, Federal Building, Asheville, N.C. 28801; also available as TN/STR-57 from National Center for Atmospheric Research].

Wallace, J. M., and V. E. Kousky, 1968: On the relation between Kelvin waves and the quasi-biennial oscillation. *J. Meteor. Soc. Japan*, **47**, 496–502.

——, and C. P. Chang, 1969: Spectrum analysis of large-scale wave disturbances in the tropical lower troposphere. *J. Atmos. Sci.*, **26**, 1010–1025.

Yanai, M., and T. Maruyama, 1966: Stratospheric wave disturbances propagating over the equatorial Pacific. *J. Meteor. Soc. Japan*, **44**, 291–294.